Maleic Anhydride Grafted Polypropylene as a Coupling Agent for Polypropylene Composites Filled with Ink-Eliminated Waste Paper Sludge Flour

Xiuying Qiao, Yong Zhang, Yinxi Zhang

Research Institute of Polymeric Materials, Shanghai Jiaotong University, Shanghai 200240, People's Republic of China

Received 19 November 2002; accepted 7 July 2003

ABSTRACT: Ink-eliminated sludge flour (IESF), a waste residue from the recycling treatment of waste paper, is a promising new kind of filler for thermoplastic polymers with a good price/performance ratio and advantages for environmental protection. In this study, high-impact polypropylene (PP) and maleic anhydride grafted polypropylene (MAPP) were chosen as a polymer matrix and a coupling agent, respectively, for the preparation of IESF/PP composites, and the structures and properties of the obtained composites were also investigated. The experimental results revealed that IESF not only induced the crystallization orientation of PP along the *b* axis but also had a restraining effect on the formation of the β phase during the recrystallization of PP from the melt; the addition of MAPP further strengthened this effect to some extent. In addition, the proper addition of MAPP was helpful for improving the thermal stability of the IESF/PP composites. With the strengthening of the interfacial interaction between the IESF and PP matrix by MAPP, the resultant efficient stress transfer from the PP matrix to the IESF particles led to increased tensile and flexural strength. However, the original greater rigidity of MAPP, with respect to PP, reduced the toughness of the composites and caused some negative effects on the impact strength and the elongation at break. © 2003 Wiley Periodicals, Inc. J Appl Polym Sci 91: 2320–2325, 2004

Key words: poly(propylene) (PP); composites; fillers; compatibility; crystallization

INTRODUCTION

Large amounts of ink-eliminated sludge are produced during the recycling treatment of waste paper, and 90% of the total waste residue in the ink-eliminated system is sludge during the recycling treatment of normally produced newspaper; this makes sludge disposal a great environmental problem. Generally, most paper sludge is landfilled, although some sludge is incinerated or used for farming. However, some research workers have recently tried to use paper sludge to fill some thermoplastic polymers such as polypropylene (PP).[1,2] In this case, many advantages, such as low cost, the disposal of industrial waste, and good mechanical properties, have been found for paper-sludge/PP composites, as described in ref. 2. Different from paper sludge, the byproduct from paper manufacturing, ink-eliminated sludge flour (IESF), derived from waste-paper recycling, contains large amounts of inorganic fillers such as kaolin, in addition to some short organic cellulose fibers. Because of its lower cost and coreinforcement of inorganic and organic fillers, IESF is probably more promising as a filler with wide commercial applications and development prospects. Most importantly, the pressure of environmental protection can be lightened, and the idea of changing waste materials into things of value for IESF can be realized.

PP, a general plastic, possesses many advantages and has been widely used in many fields of production and life. For applications, PP is usually filled with mica, talc, calcium carbonate, and glass fibers to lower the price and for property reinforcement. Meanwhile, some natural fibers, such as wood,[3–5] cellulose,[6] jute,[7] bamboo,[8,9] and conifer,[10] have been tried as new fillers for PP because of their low price, low density, high stiffness, and low abrasion during processing with respect to traditional mineral fillers. In this study, a PP copolymer with a high-impact strength was chosen as a polymer matrix, and IESF was used as a new kind of filler for the preparation of PP composites.

During the preparation of the PP composites, the improvement of the compatibility between the hydrophilic fillers and the hydrophobic PP is very important, whether the filler is an inorganic mineral or an organic fiber, because the interfacial adhesion between the filler and matrix plays an important role in determining the mechanical properties of the composites. Generally, to improve the compatibility between the filler and matrix, coupling agents such as silane, titanate, and maleic anhydride grafted polypropylene (MAPP) have been used. In this study, MAPP was

Correspondence to: Y. Zhang (yxzhang@sjtu.edu.cn).

Contract grant sponsor: Shanghai Postdoctoral Foundation.

Journal of Applied Polymer Science, Vol. 91, 2320–2325 (2004)

TABLE I
Formulations of the IESF/PP Composites[a]

Sample	PP (wt%)	MAPP (wt%)	IESF (wt%)
PP	100	0	0
MAPP0	70	0	30
MAPP1	69	1	30
MAPP3	67	3	30
MAPP5	65	5	30
MAPP10	60	10	30
MAPP20	50	20	30

[a] (PP+MAPP): IESF = 70 : 30 by weight.

used as a compatibilizer to improve the interfacial adhesion between the IESF filler and the PP matrix, and the influence of the MAPP content on the structures and properties of the IESF/PP composites was also examined.

EXPERIMENTAL

Materials

The commercial high-impact PP (B240) chosen for this study was acquired from Panjin Chemical Industry (Panjin, China). It consisted of an ethylene–propylene block copolymer, with a density of 0.91 g/cm^3 and a melt-flow index of 0.4 g/10 min (230°C and 2.16 kg). IESF was obtained after the treatment of sludge from a waste-paper recycling mill by drying, grounding, and sieving to an 80–200 mesh. The coupling agent MAPP was prepared in our laboratory by direct reactive melt extrusion, and the grafting rate was measured to be 0.3 mol %.

During the preparation of the IESF/PP composites, the IESF content was kept constant at 30 wt %, and the MAPP content was kept at 0, 1, 3, 5, 10, or 20 wt %; the obtained IESF/PP composites were designated MAPP0, MAPP1, MAPP3, MAPP5, MAPP10, and MAPP20, respectively. Table I lists the formulations of the IESF/PP composites mentioned previously. The IESF/PP composites were prepared by the use of a twin-screw extruder after the physical premixing of the components in an SHR-10A high-speed mixer (Zhangjiagang Baixiong Machinery Co., Ziangjiagang, China) for 15 min at room temperature. The temperatures of the five processing zones were 180, 185, 190, 195, and 195°C; the screw speed was 250 rpm, and the material output was 18 kg/h. After melt blending in the twin-screw extruder, the extruded strands were cooled in a cold water bath, pulled, pelletized into granules, and dried at 80°C for 3 h before injection molding. With an HFT 150 screw injection-molding machine (Ningbo Haitian Machinery Co., Ningbo, China), the composite pellets were injection-molded into ASTM standard specimens for mechanical measurements. The temperatures of the four injection zones were 220, 220, 210, and 200°C, and the injection pressure was 60 MPa. All the specimens were conditioned at 23°C for 48 h before the testing.

Measurements

X-ray diffraction investigations were performed on a Rigaku D_{max}-rC X-ray diffractometer (Japan) with Cu Kα radiation at room temperature. The measurements were carried out at 40 kV and 100 mA from 1 to 40° at a scanning rate of 10°/min with an interval of 0.02°, and the specimens for the measurements were some circular slices obtained from injection molding.

A PerkinElmer Paragon 1000 Fourier transform infrared (FTIR) spectrometer (USA) was used for to obtain detailed structural information. The specimens were thin films (ca. 30 μm thick) obtained from the hot pressing of the compounded pellets, and the FTIR spectra were recorded from 450 to 4000 cm^{-1} at room temperature.

With a PerkinElmer TGA-7 thermogravimetric analyzer, the thermal stability of the IESF/PP composites were analyzed from room temperature to 800°C at a heating rate of 20°C/min in a nitrogen atmosphere.

An Instron 4465 universal tensile tester (USA) was used to evaluate the tensile and flexural properties according to ASTM standards D638-94b and D790-92, respectively, and the crosshead speeds were 50.0 and 2.0 mm/min for the tensile and flexural measurements, respectively. During the three-point flexural testing, the support span length was kept at 50 mm. With a Ray-Ran universal pendulum impact tester (UK), the unnotched and notched Izod impact strengths were tested according to ASTM D 256-97, with a hammer weight of 0.818 kg and an impact velocity of 3.5 m/s. All the specimens were conditioned at 23°C for 48 h before being tested. In addition, a Zwick 3106 hardness tester (Germany) was used for measuring the hardness of the PP composites according to the German standard DIN EN 2039-1. Five specimens of each sample were tested to obtain the average value for the determination of the mechanical properties.

RESULTS AND DISCUSSION

Structural analysis

Figure 1 gives the X-ray diffraction patterns of the IESF/PP composites and the pure materials. The X-ray diffraction patterns of the IESF/PP composites illustrate separate characteristic diffractions of isotactic polypropylene (iPP) and IESF. PP and the IESF/PP composites exhibit four strong characteristic diffractions of the (110), (040), and (130) planes of the α phase and the (300) plane of the β phase of iPP, whereas IESF and the IESF/PP composites exhibit the characteristic

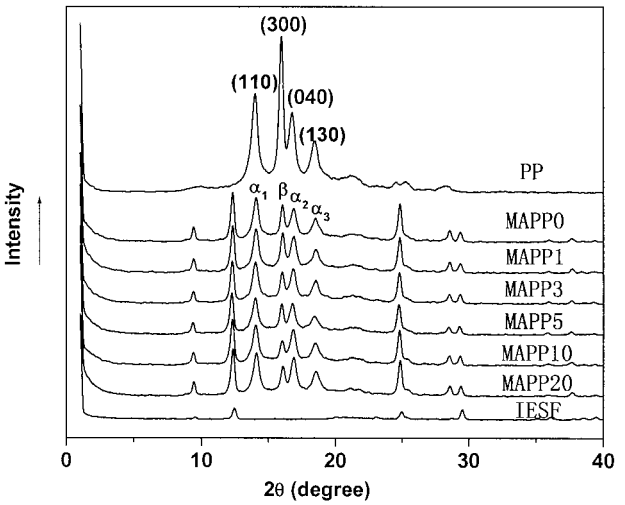

Figure 1 X-ray diffraction patterns of IESF/PP composites with different contents of MAPP.

diffractions of kaolin centered at 9.58, 12.44, 24.98, and 29.52°, respectively. As shown in Figure 1, after the blending of PP, IESF, and the MAPP coupling agent, the characteristic diffraction of PP and IESF shows almost no change in the peak position, but there is a relative change in the peak intensity for the crystalline phases of PP.

It has been reported previously that the relative amount of the β phase can be described in terms of the K value:[11]

$$K = H_\beta/[H_\beta + (H_{\alpha1} + H_{\alpha2} + H_{\alpha3})] \quad (1)$$

where $H_{\alpha1}$, $H_{\alpha2}$, and $H_{\alpha3}$ represent the heights of the characteristic diffractions of (110), (040), and (130) of the α phase and H_β represents the height of the characteristic diffraction of (300) of the β phase. According to eq. (1), K can be obtained through the calculation of the intensity proportions among the crystalline phases with reference to the experimental data from X-ray diffraction. Similarly, the relative amounts of diffraction from the different crystalline planes of the α phase can also be evaluated through the calculation of their intensity proportions to the total crystalline phase. In this study, R_1, R_2, and R_3 describe the relative amounts of diffraction from the (110), (040), and (130) crystalline planes of the α phase, respectively:

$$R_1 = H_{\alpha1}/[H_\beta + (H_{\alpha1} + H_{\alpha2} + H_{\alpha3})] \quad (2)$$

$$R_2 = H_{\alpha2}/[H_\beta + (H_{\alpha1} + H_{\alpha2} + H_{\alpha3})] \quad (3)$$

$$R_3 = H_{\alpha3}/[H_\beta + (H_{\alpha1} + H_{\alpha2} + H_{\alpha3})] \quad (4)$$

The obtained values of K, R_1, R_2, and R_3 are all listed in Table II. With respect to pure PP, the IESF/PP composites show greater relative amounts of the α phase but lower relative amounts of the β phase, indicating that the addition of IESF has a restraining effect on the formation of the β phase but a favorable effect on the formation of the α phase during the recrystallization of PP from the melt. In addition, after the addition of the MAPP coupling agent, R_2 obviously increases. Meanwhile, when the MAPP content is less than 20 wt %, R_2 keeps increasing with increasing contents of MAPP. The increasing R_2 value indicates a remarkable increase in the amount of diffraction from the (040) plane of the α phase, and this implies that the addition of MAPP further induces the crystallization orientation of PP along the b axis. From Table II, it can also be observed that when the MAPP content is 10 wt %, the relative amounts of the α phase and β phase reach their maximum and minimum separately. Thus, a certain MAPP addition not only strengthens the crystallization orientation of iPP along the b axis but also has a further restraining effect on the crystallization of the β phase of iPP.

The effects of the IESF filler and the MAPP coupling agent on the formation of the crystalline phases of PP in the composites can also be described by the change in the crystallite size (L_{hkl}), which represents the mean dimension of crystallites perpendicular to planes *hkl* and can be calculated according to the Sherrer equation.[12] The crystallite sizes of the crystalline phases of

TABLE II
The Crystalline Parameters of the PP and IESF/PP Composites

	α-phase						β-phase	
Sample	L_{110} (nm)	R_1	L_{040} (nm)	R_2	L_{130} (nm)	R_3	L_{300} (nm)	K
PP	12.07	0.256	3.41	0.208	7.00	0.137	19.41	0.399
MAPP0	13.76	0.315	8.85	0.241	8.87	0.175	17.60	0.269
MAPP1	13.78	0.302	10.78	0.254	9.28	0.168	17.80	0.277
MAPP3	13.78	0.312	11.40	0.265	9.74	0.182	18.00	0.241
MAPP5	14.84	0.304	12.11	0.269	7.50	0.159	19.40	0.268
MAPP10	12.87	0.322	11.41	0.291	8.87	0.185	14.87	0.202
MAPP20	12.87	0.315	11.40	0.281	9.28	0.185	14.87	0.219

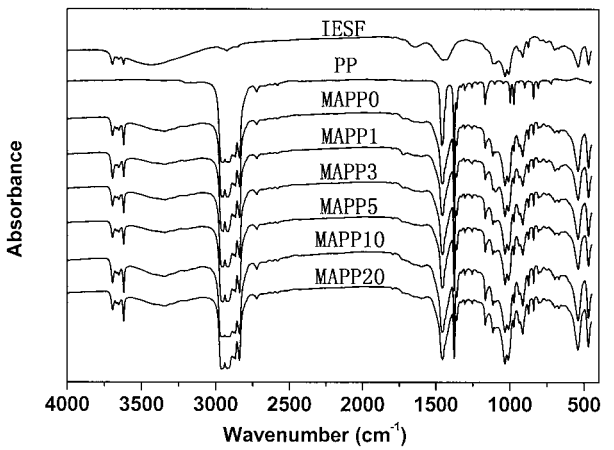

Figure 2 FTIR spectra of IESF/PP composites with different contents of MAPP.

PP for the unfilled PP and IESF/PP composites are also listed in Table II. The IESF/PP composites possess a greater crystallite size for the α phase but a smaller size for the β phase than unfilled PP, especially L_{040}. Thus, the addition of IESF not only has positive and negative effects on the crystal growth of the α phase and β phase, respectively but also induces the crystallization orientation of PP along the *b* axis because of its nucleation agent, as reported previously.[11] Moreover, after MAPP is added, some increase in the crystallite size occurs for both the α phase and β phase at first, but the crystallite size begins to decrease when the MAPP content increases to a certain extent. From this analysis, it can be found that the MAPP coupling agent can strengthen the nucleation agent effect of IESF and be helpful for the crystal growth of PP to some degree.

Infrared spectroscopy

FTIR experiments were performed on the IESF/PP composites and the pure components to obtain detailed structural information and to examine the bond interactions within the composites; the obtained FTIR spectra are shown in Figure 2. Similarly to the X-ray diffraction experiments, the IESF/PP composites show separate characteristic absorbance peaks of IESF and PP, and the absorbance peaks almost remain at the same position. However, after the blending of PP and IESF, the stretching vibrations of —OH at 3344 cm^{-1} and absorbed water in the 1650–1600-cm^{-1} region undergo a decrease in intensity, but the further effects of the MAPP coupling agent on the absorbance peaks are not obvious. In Figure 2, the characteristic peaks of the MA group at 1865, 1788, and 1717 cm^{-1} cannot be observed for the IESF/PP composites with the addition of MAPP, which may provide advantageous support for the interactions between the hydroxyl groups of the fillers and the polar MA groups of the coupling agent.[13]

Thermogravimetric analysis

The results of the thermogravimetric analysis of the IESF/PP composites are shown in Figure 3. The moisture content of IESF is 4.0 wt %, and the contents of the organic and inorganic materials are 46.4 and 49.6 wt %, respectively. In general, in ink-eliminated wastepaper sludge, the main component of the organic material is short cellulose fibers, and that of the inorganic material is kaolin. As shown in Figure 3, after the addition of MAPP, the PP composites exhibit higher onset degradation temperatures with better thermal stability. According to the experimental results, the onset degradation temperatures are 396.05, 415.64, 462.26, 458.16, 458.95, 461.17, and 461.18°C for PP, MAPP0, MAPP1, MAPP3, MAPP5, MAPP10, and MAPP20, respectively. It seems that the proper addition of the MAPP coupling agent is helpful for improving the thermal stability of the IESF/PP composites.

Mechanical properties

The mechanical properties of the IESF/PP composites are given in Table III. After the blending of the IESF filler with PP, the impact strength and tensile strength decrease and the flexural strength and hardness increase, with respect to unfilled PP. The decrements of the notched impact strength and the tensile strength are 92 and 11%, respectively, and the increments of the flexural strength, flexural modulus, and hardness are 6, 31, and 22%, respectively. After the incorporation of the MAPP coupling agent, the IESF/PP composites

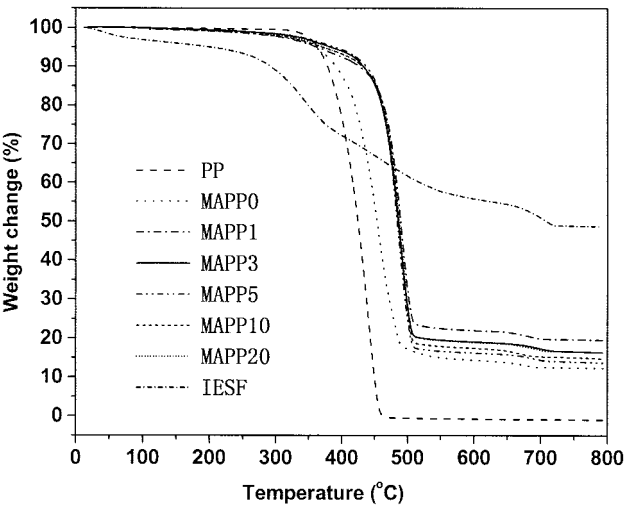

Figure 3 Results of the thermogravimetric analysis of IESF/PP composites with different contents of MAPP.

TABLE III
The Mechanical Properties of the IESF/PP Composites

Sample	Izod Impact strength (unnotched, J/m)	Izod Impact strength (notched, J/m)	Tensile strength (MPa)	Flexural strength (MPa)	Flexural modulus (MPa)	Hardness (N/mm^2)
PP	No Break	852	26.9	29.5	960	51.6
MAPP0	633	67.6	24.0	31.4	1259	63.0
MAPP1	535	53.6	25.4	33.0	1296	63.1
MAPP3	557	54.6	26.4	33.7	1328	63.4
MAPP5	617	58.8	27.3	34.9	1406	63.6
MAPP10	595	55.8	28.2	36.1	1446	66.7
MAPP20	569	51.6	29.9	39.0	1581	71.7

undergo a further decrease in the unnotched and notched impact strength but a further increase in the tensile strength, flexural strength and modulus, and hardness. Generally, MAPP, as a reactive coupling agent, is used as a compatibilizer because it can efficiently improve fiber–matrix bonding on account of the formation of covalent linkages and hydrogen bonds between maleic anhydride and the hydroxyl groups of the fiber.[13] With the strengthening of the interfacial interaction between IESF and the PP matrix by MAPP, the resultant efficient stress transfer from the PP matrix to the IESF particles leads to an increase in the tensile and flexural strength, as reflected in the experimental results. However, the original greater rigidity of MAPP, with respect to PP, reduces the toughness of the composites and causes some negative effects on the impact strength.

The changes in the mechanical properties of the IESF/PP composites with the MAPP content are shown in Figure 4. With an increase in the MAPP content, the unnotched and notched impact strength continues increasing until a 5 wt % MAPP content and then decreases constantly, whereas the tensile and flexural strength continues increasing until a 20 wt % MAPP content. Meanwhile, with an increase in the MAPP concentration, the elongation at break continues decreasing, whereas the hardness of the composites continues increasing, because of the increase in the stiffness of the composites after the addition of the coupling agent. According to some references, improved interfacial adhesion with MAPP leads to an increase in the modulus of the composites, but it generally cause a dramatic decrease in the elongation at break.[3,14] When the amount of the MAPP coupling agent is large, the interfacial adhesion between the filler and the polymer is so strong that the debonding process becomes more difficult, and this strong effect of MAPP will inevitably result in an increase in the amount of brittle failure and a decrease in the impact strength. In addition, the strong interaction between the filler and MAPP also reinforces the tensile strength and antideformability with increasing surface coverage, and this causes an increase in the tensile strength and a decrease in the elongation at break. In most cases, once the material becomes harder and stiffer, the elongation at break is inevitably lowered. Similarly to the Myers research group,[15] we have found that the

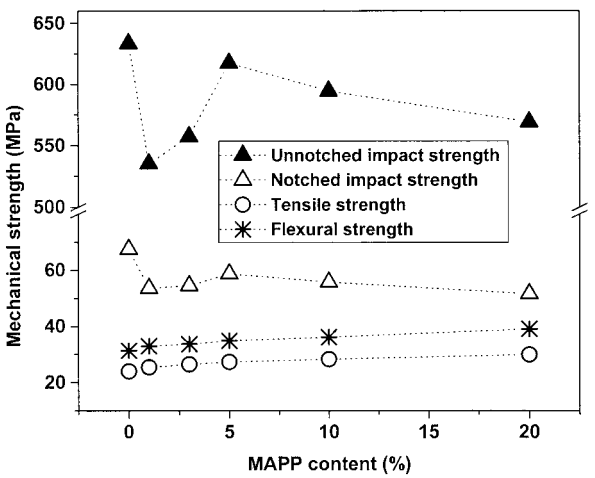

(a)

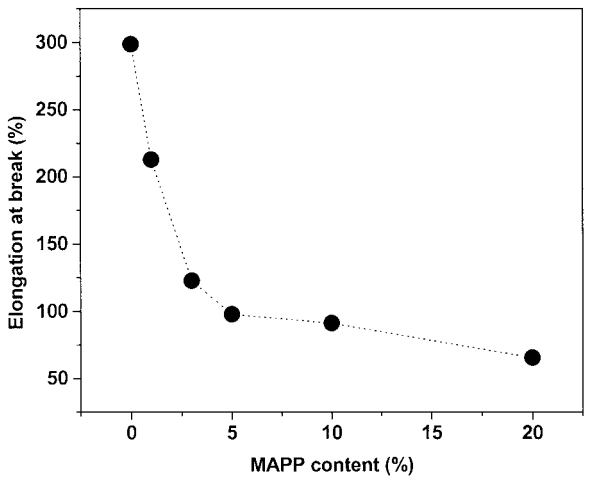

(b)

Figure 4 Effects of the MAPP concentration on the mechanical properties of IESF/PP composites: (a) the mechanical strength and (b) the elongation at break.

use of the MAPP coupling agent does not greatly enhance the impact strength by more energy dissipation when the fibers are pulled out of the matrix. This phenomenon is probably attributable to the clustering of the fibers and the existence of large amounts of inorganic kaolin in IESF. The somewhat badly separated fibers and the existence of an inorganic filler in a great amount probably form some defect points in the polymer matrix, thus causing some gaps between the fiber and matrix and the resultant brittleness of the composites. Therefore, the morphological features of the fillers strongly influence their dispersion in the polymeric matrix, the wettability of their particles by the polymeric matrix, and the mechanical properties of the composites.

CONCLUSIONS

The measurements of both X-ray diffraction and FTIR imply that there is no obvious interaction between IESF and PP with their separate characteristic diffractions and absorbances. During the recrystallization of PP from the melt, the IESF filler not only has favorable and restraining effects on the formation of its α phase and β phase, respectively, but also induces its crystallization orientation along the b axis. Meanwhile, a certain MAPP addition will strengthen the crystallization orientation of PP along the b axis and have a further restraining effect on the crystallization of the β phase of PP. The thermogravimetric analysis results reveal that the proper addition of the MAPP coupling agent is helpful for improving the thermal stability of the IESF/PP composites. After the blending of the IESF filler and PP, the impact and tensile strength decreases and the flexural strength and hardness increase, with respect to unfilled PP. As a reactive coupling agent, MAPP leads to an increase in the tensile and flexural strength by strengthening the interfacial interaction between IESF and the PP matrix, but it reduces the toughness of the composites and causes some negative effects on the impact strength and the elongation at break at the same time because of its original greater rigidity, with respect to PP.

The authors thank Shanghai Nuo Ya Environmental Resources Exploitation Co., Ltd., for the supply of paper sludge flour.

References

1. Son, J.; Kim, H.-J.; Lee, P.-W. J Appl Polym Sci 2001, 82, 2709.
2. Jang, J.; Lee, E. Polym Test 2001, 20, 7.
3. Oksman, K.; Clemons, C. J Appl Polym Sci 1998, 67, 1503.
4. Ichazo, M. N.; Albano, C.; Gonzalez, J.; Perera, R.; Candal, M. V. Comp Struct 2001, 54, 207.
5. Wu, J. S.; Yu, D. M.; Chan, C.-M.; Kim, J.; Mai, Y.-W. J Appl Polym Sci 2000, 76, 1000.
6. Amash, A.; Zugenmaier, P. Polym Bull 1998, 40, 251.
7. Gassan, J.; Bledzki, A. K. Compos A 1997, 28, 1001.
8. Mi, Y. L.; Chen, X. Y.; Guo, Q. P. J Appl Polym Sci 1997, 64, 1267.
9. Chen, X. Y.; Guo, Q. P.; Mi, Y. L. J Appl Polym Sci 1998, 69, 1891.
10. Chuai, C. Z.; Almdal, K.; Poulsen, L.; Plackett, D. J Appl Polym Sci 2001, 80, 2833.
11. Alonso, M.; Velasco, J. I.; de Saja, J. A. Eur Polym J 1997, 33, 255.
12. Hsieh, Y. L.; Mo, Z. S. J Appl Polym Sci 1987, 33, 1479.
13. Feng, D.; Caulfield, D. F.; Sanadi, A. R. Polym Compos 2001, 22, 506.
14. Demjen, Z.; Pukanszky, B. Polym Compos 1997, 18, 741.
15. Myers, G. E.; Chahyadi, I. S.; Coberly, C. A.; Ermer, D. S. Int J Polym Mater 1991, 15, 21.